Microfabrication and application of high-aspect-ratio silicon tips

Yaqiang Wang and Daniel W. van der Weide
Department of Electrical and Computer Engineering, University of Wisconsin, Madison, Wisconsin 53706

(Received 1 February 2005; accepted 9 May 2005; published 21 July 2005)

We report a new process combining reactive ion etching (RIE) and deep RIE (DRIE) tools for microfabrication of high-aspect-ratio (HAR) silicon tips with heights $>$40 μm and aspect ratios of 7. We integrate atomic force microscope (AFM) cantilevers with HAR tips and compare AFM scans using an HAR tip and a commercial tip. Our results demonstrate the advantage of HAR tips for metrology applications. © *2005 American Vacuum Society.* [DOI: 10.1116/1.1947805]

I. INTRODUCTION

High-aspect-ratio (HAR) atomic force microscope (AFM) tips are needed for deep access in the semiconductor industry[1] and metrology of Microelectromechanical Systems (MEMS) structures.[2] There are currently three means to fabricate HAR tips: ultrasharp silicon tips;[3–5] attaching carbon nanotubes to regular AFM tips;[6–8] and using focused ion beam (FIB) milling to make supertips.[9,10] These methods involve complex process procedures, high costs, and inability to achieve tip heights taller than 30 μm. We have designed a batch process for the microfabrication of HAR silicon tips with heights taller than 40 μm (potentially $>$100 μm) and aspect ratios of 7. The fabrication method reported here differs from previous methods in the comparably low cost, good reproducibility, and super tip height.

II. PROCESS

A. HAR tip

The HAR tip process is outlined in Fig. 1. First, a 1-μm-thick thermal oxide is grown on a Si (100) wafer. Then a 16-μm-diam oxide disk is patterned by standard photolithography and buffered hydrofluoric (BHF) acid etch [Fig. 1(a)]. The exposed Si is etched by RIE (SF$_6$, 45 sccm, 100 W) to form a tip precursor that will determine the final tip shape [Fig. 1(b)]. Next, a DRIE process is performed using a commercial STS® Multiplex ICP system (Surface Technology Systems, Redwood, CA) to form a tip shaft. The process starts from a C$_4$F$_8$ deposition (95 sccm, 6 s, APC 66°, RF 600 W), which alternates with SF$_6$ etching steps (130 sccm, 8 s, APC 66°, RF 600 W). Because DRIE generates characteristic scalloping features on the sidewall of the tip shaft,[11] an SF$_6$/O$_2$ etching step (SF$_6$ 45 sccm, O$_2$ 5 sccm, 100 W) is used to smooth the sidewall. Then the oxide disk is removed with hydrofluoric acid [Fig. 1(c)]. Finally, the tip is sharpened by oxidation sharpening steps at 950 °C.[12,13] Figure 2(a) shows an SEM micrograph of a microfabricated HAR tip using this method. The height of the tip is 42 μm with an aspect ratio of 7 (the ratio of tip height to tip width). Figure 2(b) is a close view of a HAR tip, whose tip radius is estimated to be 10 nm. The tips fabricated on a single wafer chip had heights 40 μm$\pm$2 μm, and were repeated for multiple runs. The major process cost comes from STS DRIE process, which is comparably low with high silicon etch rate and batch process. The tip height can be larger than 100 μm using this method, and limitation only lies in the selectivity of silicon over silicon dioxide mask during RIE and DRIE steps.

B. AFM probe with HAR tip

Batch fabrication of AFM probes integrated with HAR tips is illustrated in Fig. 3. The process starts with a Si$_3$N$_4$ film deposition on a Si (100) wafer by LPCVD [Fig. 3(a)]. Then windows are opened on the backside of the wafer by photolithography and RIE. The wafer is etched in KOH solution to form the probe chip bodies [Fig. 3(b)]. After stripping the Si$_3$N$_4$ films, the cantilever is patterned by photolithography [Fig. 3(c)]. The cantilever thickness is etched by RIE using photoresist (PR) as a mask layer [Fig. 3(d)]. Next, an HAR tip is fabricated using the aforementioned method after the growth of a 1-μm thermal oxide [Figs. 3(e) and 3(f)]. The distance from the tip to the cantilever end is set to be 20 μm by considering the horizontal undercut during the STS DRIE step. The AFM probe is released by a backside RIE with a thick PR coating on the front side of the wafer [Fig. 3(g)]. Figure 4 shows two SEM micrographs of a mi-

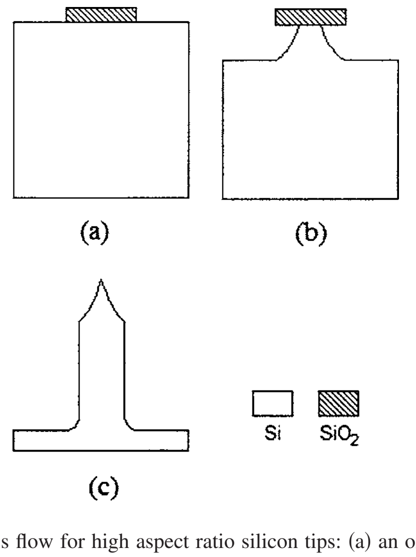

FIG. 1. Process flow for high aspect ratio silicon tips: (a) an oxide tip mask is etched by BHF; (b) the tip mask is undercut by an SF$_6$ RIE; (c) the tip shaft is anisotropically etched by STS DRIE process, smoothed by SF$_6$/O$_2$ RIE, and the final tip is released by SF$_6$ RIE plus an HF etching.

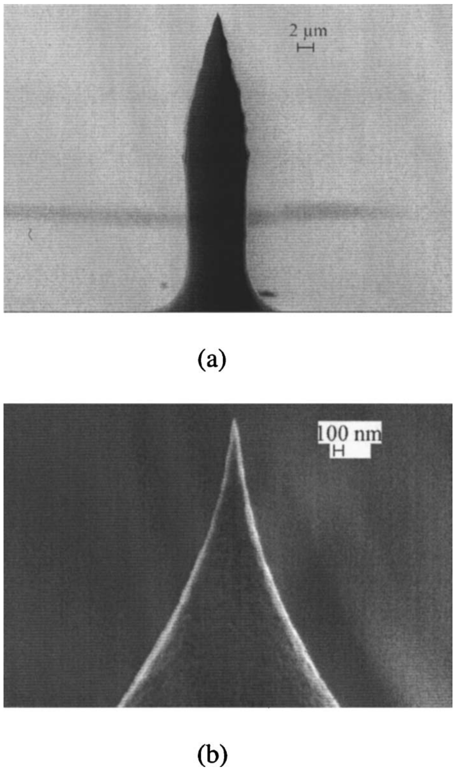

FIG. 2. SEM micrographs of HAR tips: (a) a tip with a height of 42 μm and an aspect ratio of 7; (b) a tip with a tip apex radius of 10 nm.

crofabricated AFM probe with a HAR tip. Figure 4(a) is a perspective view of the AFM probe. A close view of the tip in Fig. 4(b) shows a tip height of 32 μm with an aspect ratio of 8.

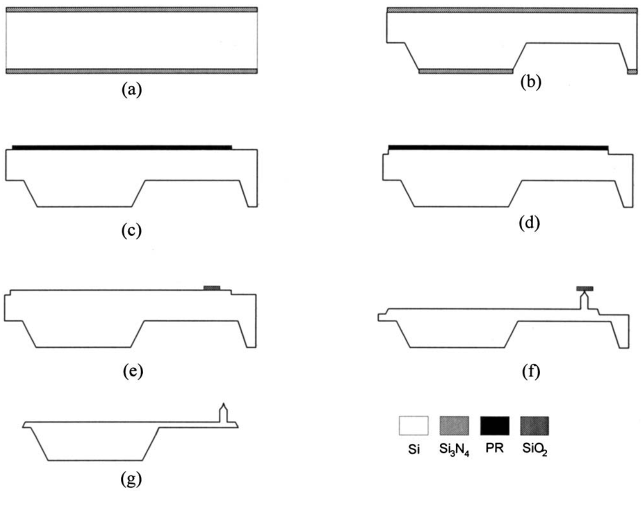

FIG. 3. Process flow for microfabrication of AFM probes integrated with high-aspect-ratio tips: (a) LPCVD Si_3N_4 150 nm; (b) chip body is etched by KOH (30 wt. %, 80 °C); (c) photolithography to pattern the cantilever structure; (d) the cantilever thickness is etched by SF_6/O_2 RIE; (e) 1-μm thermal oxide growth and tip mask patterning by BHF etching; (f) HAR tip etching; (g) AFM probe release by a backside SF_6 RIE.

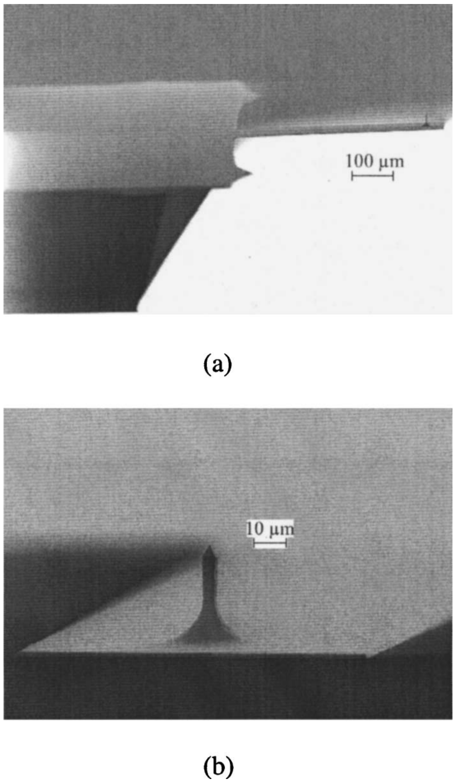

FIG. 4. SEM micrographs of an AFM probe with a HAR tip. (a) Perspective view of the AFM probe with the HAR tip; (b) close view of the HAR tip with a height of 32 μm and an aspect ratio of 8.

III. APPLICATION

We performed noncontact scans of a polydimethylsiloxane (PDMS) sample with an array of holes using a commercial Topometrix Explorer AFM system. The AFM probe in Fig. 4 and a commercial noncontact AFM probe were both used for the same scans as a comparison. The commercial AFM probe has a tip height of 15 μm and an aspect ratio of 1.5, as shown in Fig. 5. Figure 6(a) shows the topography using the AFM probe with HAR tip while Fig. 6(b) is the image using the commercial probe. From line measurements across holes with the same dimension, the resolved depth of

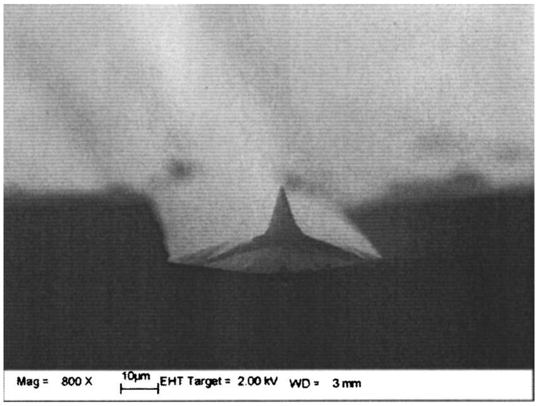

FIG. 5. SEM micrograph of a commercial AFM tip with a height of 15 μm and an aspect ratio of 1.5.

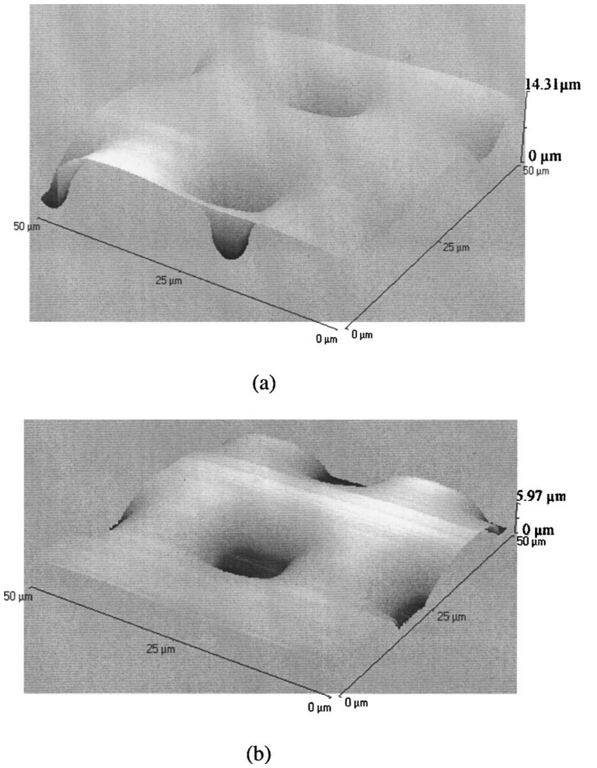

FIG. 6. Noncontact-mode AFM images of a PDMS sample with holes: (a) AFM scan using the tip of Fig. 4; (b) AFM scan using the tip of Fig. 5.

the holes is around 11.5 μm in Fig. 6(a), and only 4.5 μm in Fig. 6(b). Figure 7 shows the overlay of both measurements, in which the curve scanned by the commercial tip is vertically shifted to be the same level as the curve by the HAR tip. It is clear that the profiles of the holes from the two AFM measurements are almost the same, while the HAR tip resolves the depth more accurately. The scan by the commercial AFM tip was limited by its low aspect ratio, demonstrating the advantage of the HAR tip in this application. Since typical stylus profilers cannot resolve features with several microns due to the size of the metal stylus, and typical AFM measurements only resolve features with heights of several microns, the HAR tips in this work can be used for MEMS metrology to measure the topography, surface smoothness, and high resolution of three-dimensional images of MEMS devices with heights up to tens of microns. Another important application of HAR tips is for AFM-compatible scanning near-field microwave microscopy.[14] A coaxial HAR tip with super height will greatly reduce the parasitic capacitive coupling between the cantilever and sample, therefore improving the sensitivity.[15]

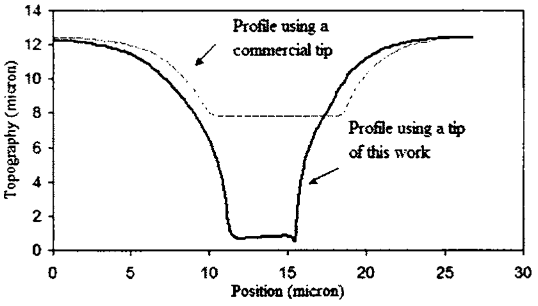

FIG. 7. Overlay of line measurement profiles for two AFM scans with different tips.

ACKNOWLEDGMENT

This work has been supported by AFOSR MURI03 with Grant No. F49620-03-1-0420.

[1] S. Hosaka, T. Morimoto, H. Kuroda, Y. Minomoto, Y. Kembo, and H. Koyabu, Appl. Surf. Sci. **188**, 467 (2002).
[2] Application notes from Veeco Metrology Group, Santa Barbara, CA, USA.
[3] I. W. Rangelow, F. Shi, P. Hudek, P. Grabiec, B. Volland, E. I. Givargizov, A. N. Stepanova, L. N. Obolenskaya, E. S. Mashkova, and V. A. Molchanov, J. Vac. Sci. Technol. B **16**, 3185 (1998).
[4] E. I. Givargizov, A. N. Stepanova, L. N. Obolenskaya, E. S. Mashkova, and V. A. Molchanov, M. E. Givargizov, and I. W. Rangelow, Ultramicroscopy **82**, 57 (2000).
[5] J. Thaysen, A. Boisen, O. Hansen, and S. Bouwstra, Sens. Actuators, A **83**, 47 (2000).
[6] A. Olbrich, B. Ebersberger, C. Bit, Ph. Niedermann, W. Hänni, J. Vancea, and H. Hoffman, J. Vac. Sci. Technol. B **17**, 1570 (1999).
[7] S. Rozhok, S. Jung, V. Chandrasekhar, X. Lin, and V. P. Dravid, J. Vac. Sci. Technol. B **21**, 323 (2003).
[8] A. B. H. Tay and J. T. L. Thong, Appl. Phys. Lett. **84**, 5207 (2004).
[9] T. Morimoto, H. Kuroda, Y. Minomoto, Y. Nagano, Y. Kembo, and S. Hosaka, Jpn. J. Appl. Phys., Part 1 **41**, 4238 (2002).
[10] A. Olbrich, B. Ebersberger, C. Boit, Ph. Niedermann, W. Hänni, J. Vancea, and H. Hoffmann, J. Vac. Sci. Technol. B **17**, 1570 (1999).
[11] A. A. Ayón, R. Braff, C. C. Lin, H. H. Sawin, and M. A. Schmidt, J. Electrochem. Soc. **146**, 339 (1999).
[12] Yongxia Zhang, Yanwei Zhang, T. S. Sriram, and R. B. Marcus, Appl. Phys. Lett. **69**, 4260 (1996).
[13] R. B. Marcus, T. S. Ravi, T. Gmitter, K. Chin, D. Liu, W. J. Orvis, D. R. Ciarlo, C. E. Hunt, and J. Trujillo, Appl. Phys. Lett. **56**, 236 (1990).
[14] D. W. van der Weide, Appl. Phys. Lett. **70**, 677 (1997).
[15] M. Tabib-Azar and Y. Wang, IEEE Trans. Microwave Theory Tech. **52**, 971 (2004).